Hindawi
International Journal of Antennas and Propagation
Volume 2019, Article ID 3209840, 9 pages
https://doi.org/10.1155/2019/3209840

Research Article

A Compact Wideband Printed Antenna for 4G/5G/WLAN Wireless Applications

Ming Yang,[1,2] Yufa Sun ,[1] and Fan Li[1]

[1]*Key Lab of Intelligent Computing and Signal Processing, Ministry of Education, Anhui University, No. 111, Jiulong Road, Jingkai District, Hefei 230601, China*
[2]*Electronics and Information Engineering Department, Bozhou University, No. 2266, Tangwang Road, Jingkai District, Bozhou 236800, China*

Correspondence should be addressed to Yufa Sun; yfsun_ahu@sina.com

Received 26 January 2019; Revised 3 July 2019; Accepted 17 July 2019; Published 10 September 2019

Guest Editor: Abhinav Kumar

A compact wideband printed antenna with deca-band 4G/5G/WLAN for mobile phone devices is proposed in this paper. The complete structure is composed of a monopole antenna and a coupling strip, occupying a small C-shape PCB area of $27 \times 10.8\,\mathrm{mm}^2$. This antenna, which is printed on FR4 substrate with 0.8 mm thickness and fed by a coaxial cable, can provide three wide operating bandwidths that cover 685–1012 MHz, 1596–2837 MHz, and 3288–3613 MHz for 4G/5G/WLAN communication systems. The gains and total radiation efficiencies of the antenna in the low, middle, and high bands are 1.4 dBi–2.5 dBi and 38%–47%, respectively. Besides, the measured results are in good agreement with the simulated results. Further experiments demonstrate that the proposed antenna exhibits a good performance for mobile phones.

1. Introduction

Rapid development of the wireless communication systems, especially the wide use of 2G/3G/4G devices and mobile phone antennas with small sizes and wide operating bands, are more attractive for practical applications. As a particular case, a compact wideband printed mobile phone antenna, covering the LTE (Long-Term Evolution) 700, GSM (Global System for Mobile Communications) 850, GSM900, DCS (Digital Cellular System) 1800, PCS (Personal Communications Service) 1900, UMTS (Universal Mobile Telecommunications System) 2100, LTE2300, LTE2500, and 5G (3300–3600 MHz), is of interest. As is well known, these mobile phone antennas need to be able to operate at a wider scope of different frequencies and work in a very limited space.

Recently, various techniques have been proposed for the design of the multiband or broadband antenna. Several printed wideband antennas for mobile phones have been proposed in the literature [1–6]. However, in order to cover the LTE/WWAN (Wireless Wide Area Network) operation in the 700 MHz band, the radiating board in the printed monopole occupies a large volume, which may be folded to achieve a compact size in the mobile phone. Several techniques have been reported to widen the bandwidth and reduce the occupied space, including the multiple branches technique [7, 8], the reconfigurable method [9, 10], and the lumped-element matching method [11–14]. Another popular technique is the coupled-fed method [15, 16], which provides a convenient matching tuning mechanism. However, these methods cannot simultaneously meet both requirements of wideband operation and compact size. Therefore, it is an interesting challenge to design a wideband and compact mobile phone antenna.

In this paper, a deca-band printed antenna for 4G/5G/WLAN mobile phones with the size of $27 \times 10.8 \times 0.8\,\mathrm{mm}^3$ is proposed. A C-shaped ground plane is introduced in this paper to enhance the operating bandwidth of the antenna that is disposed on the C-shaped system circuit board, and the C-shaped ground plane is easier to adjust bandwidth than the antenna that is disposed on the conventional simple system circuit board. The proposed antenna is composed of a monopole antenna and a staircase-shape coupled ground strip. Owing to the coupling interactions, the feeding strip and the parasitic elements may generate multiple resonant modes with the help of the system ground plane. The antenna presents a measured S_{11} of lower than −6 dB inside the operation bandwidths of LTE700 (704–787 MHz), GSM850 (824–894 MHz), GSM900 (890–960 MHz), DCS (1710–1880 MHz), PCS (1850–1990 MHz), UMTS2100 (1920–2170 MHz), LTE2300 (2305–2400 MHz), and LTE2500 (2500–2690 MHz), meanwhile lower than −10 dB inside the operation bandwidths of WLAN (2400–2484 MHz) and 5G (3300–3600 MHz).

2. Antenna Geometry

The configuration of the proposed antenna is illustrated in Figure 1. Figure 1(a) shows the structure of the proposed antenna fabricated on a C-shaped FR4 substrate with a size of $120 \times 60\,mm^2$, a relative permittivity of 4.4, a thickness of 0.8 mm, and a loss tangent of 0.02. The dimensions of the proposed antenna are $27 \times 10.8\,mm^2$, located at the lower left edge of the substrate. The selected dimensions of the overall circuit board and the antenna are reasonable for practical mobile phones. The proposed antenna consists of a monopole antenna, a staircase-shaped coupled ground strip, and a 6.8 nH inductor, as shown in Figure 1(b). The driven strip, coupled ground strip, and ground plane are printed on the front side of the substrate. In the proposed antenna, the driven strip is connected (point A) to the ground plane by a 50 Ω coaxial cable, and the coupled strip is connected directly to the ground plane (point B) on the same side.

The driven strip is composed of four branches, strips 1, 2, 3, and 4, as shown in Figure 1(b), which contributes the resonant modes at lower and higher frequency bands. By adding the staircase-shaped coupled ground strip, the interaction between the driven strip and the coupled strip may generate another resonant mode around 2260 MHz, thereby improving the impedance matching and widening the middle bandwidth. To enhance the bandwidth of the middle and high band, an inductor is introduced to create two resonant frequencies around 2740 MHz and 3450 MHz. The proposed antenna is studied and discussed in detail in next section.

3. Antenna Design and Analysis

3.1. Antenna Design. In order to meet the requirements of the modern mobile phone with the deca-band 4G/5G/WLAN operation, the proposed antenna must provide multiple resonances. For convenient explanation, comparison of the simulated S_{11} of various geometric structures of the antenna is shown in Figure 2. First, antenna #1 is a monopole antenna, which generates a resonant mode only at a frequency of 1390 MHz. Next, strip 2 is added to the antenna #1, which forms antenna #2. Note that three resonant modes are excited at 672 MHz, 986 MHz, and 3752 MHz, and the impedance matching is good in the resonant modes. The antenna #3 is composed of a staircase-shaped coupled ground strip and antenna #2, which excites another resonant mode and enhances the bandwidth as 1610–2580 MHz. The antenna #4 is formed by inserting strip 3 in antenna #3. The two resonances of the lower band are shifted to the left, while the resonance of the higher band is shifted to the right. However, the corresponding bandwidths for these resonances are not wide enough to cover the whole frequency bands for LTE/WWAN/WLAN/5G.

Next, as antenna #5, an inductor is introduced in antenna #4 to enhance the bandwidth. Two resonant modes are excited at 2740 MHz and 3450 MHz with a good impedance matching. The middle and high bands cover DCS/PCS/UMTS/LTE2300/2500 and 5G (3300–3600 MHz). The lower bands LTE700/GSM850 can also be covered by optimizing the inductance.

To achieve a wide coverage in the 900 MHz band, a meander line (strip 4) is inserted into antenna #5, that is, the proposed antenna. The resonant frequency in the low band is split into three modes. Consequently, the proposed antenna may cover the LTE700, GSM850, and GSM900.

Here, we employ HFSS (high-frequency structure simulator) full-wave simulator to optimize the antenna configuration and achieve its surface current and gain. The optimized design parameters have been determined and listed in Table 1.

3.2. Parametric Analysis. In the design of this antenna, the value of the inductor L and the length of $H6$ are changed, respectively, and their effects on each resonant mode are shown in Figures 3 and 4. It can be seen in Figure 3 that the antenna's bandwidths are affected when a smaller or bigger value of L is selected, especially for the antenna's middle and high bands. In Figure 4, the results of the simulated S_{11} for the length $H6$ varying from 12.7 to 16.7 mm are presented. Relatively remarkable effects on the resonant modes in the low and middle bands are observed. Other resonant modes are generally insensitive to the length of $H6$.

4. Simulation and Measurement

Figure 5 shows the fabricated prototype of the proposed antenna, which is fed by a 50 Ω coaxial cable. S_{11} of the antenna is measured by using an Agilent N5247A vector network analyzer. The simulated and measured S_{11} are plotted in Figure 6. It may be observed that the simulated and measured results in lower and higher bands are in good agreement, while there is a small discrepancy between the simulation and measurement results in the middle band, which may be mainly due to the fabrication inaccuracy of the antenna prototype. According to −6 dB reflection coefficients, the measured impedance bandwidths of the antenna for lower and middle bands were 685–1012 MHz and 1596–2837 MHz, respectively. Meanwhile, the measured impedance bandwidths lower than −10 dB for WLAN and 5G (3300–3600 MHz) were 2146–2568 MHz and 3288–3613 MHz. Thus, the proposed antenna provides all ten operating bands, i.e., LTE700/2300/2500, GSM850/900/1800/1900/UMTS2100/WLAN, and 5G (3300–3600 MHz).

To further comprehend the resonant mechanisms of the proposed antenna, the surface current distributions are simulated in Figure 7. As shown in Figure 7(a), the surface current at 740 MHz is distributed along the longer strip (E-F-G-H) and the staircase-shaped coupled ground strip (E-C), which can provide a 0.25-wavelength resonant mode (for M_1). By observing Figure 7(b), the surface current distributes

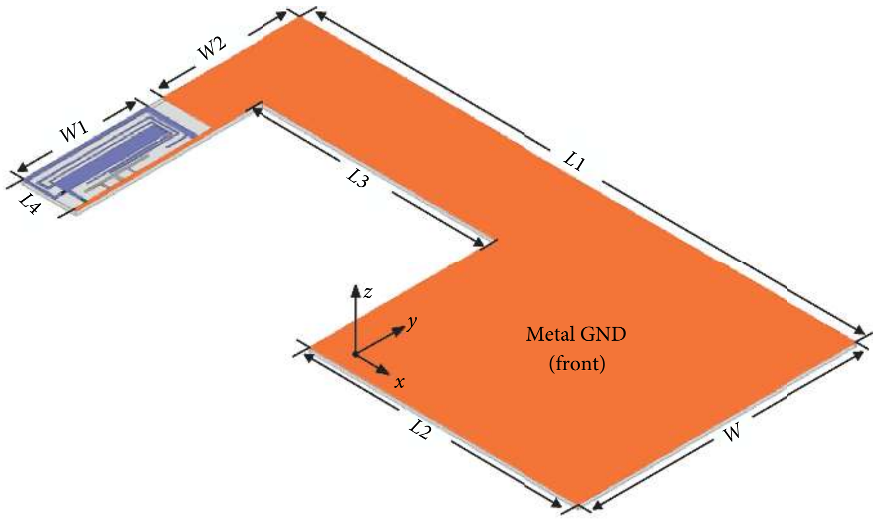

(a)

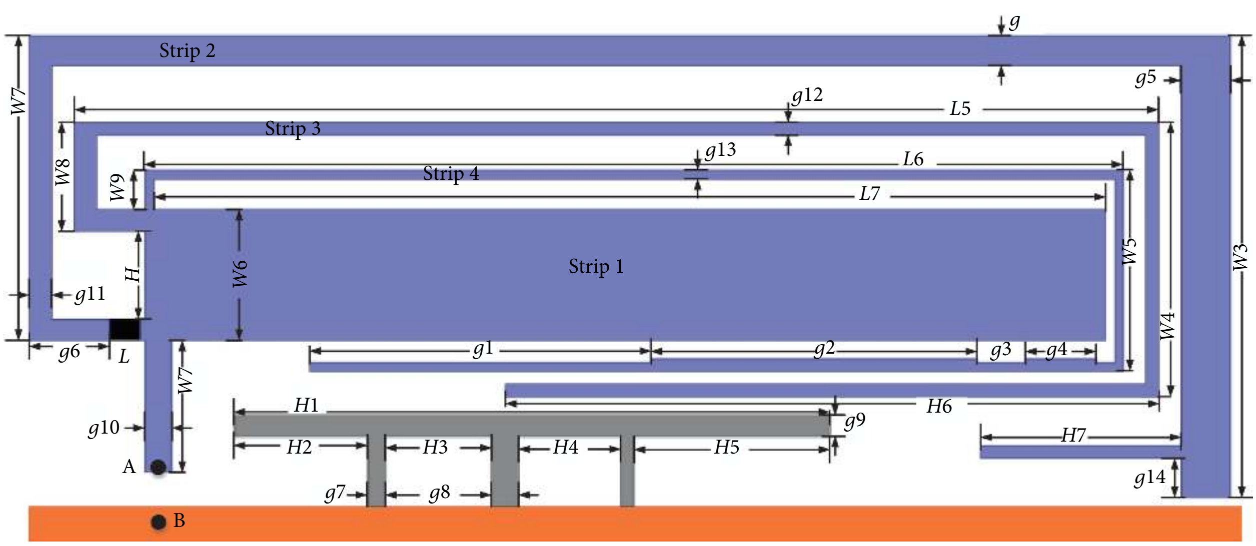

(b)

FIGURE 1: Geometry of the proposed antenna. (a) The overall structure of the proposed antenna and (b) the important part structure of the proposed antenna.

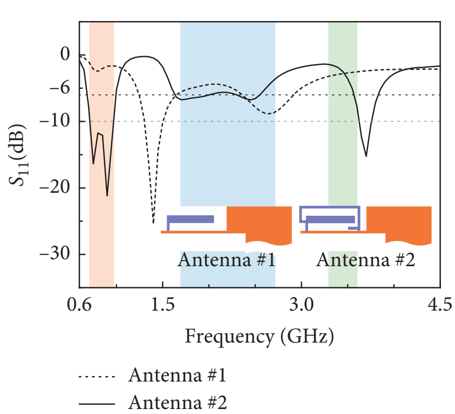

(a)

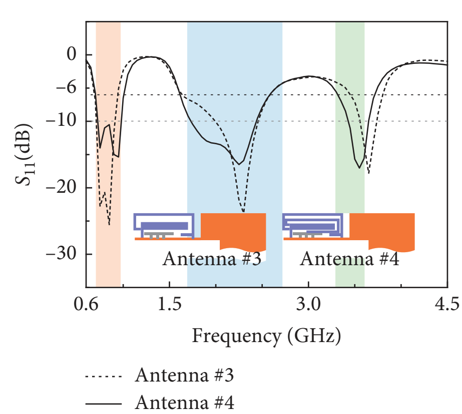

(b)

FIGURE 2: Continued.

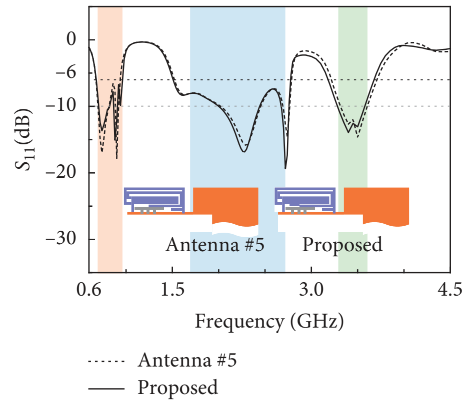

(c)

FIGURE 2: Simulation results of the S_{11} for the different antennas.

TABLE 1: Geometric parameters for the proposed antenna (unit: mm).

Parameter	Value
W	60.0
$W1$	27.0
$W2$	30.0
$L1$	120.0
$L2$	58.0
$L3$	50.4
$L4$	10.8
$W3$	10.6
$W4$	6.3
$W5$	4.6
g	0.7
$g3$	1.1
$g4$	1.6
$g2$	7.3
$H7$	4.5
$H6$	14.7
$L5$	24.4
$L6$	22.0
$L7$	21.4
$H1$	13.4
$H2$	3.0
$H3$	2.4
$H4$	2.3
$H5$	4.4
$g1$	7.7
$g6$	1.8
$g7$	0.4
$g8$	0.6
$g5$	1.1
$g9$	0.5
$W6$	3.0
$W7$	7.0
$W8$	2.5
$W9$	0.9
H	2.0
$g10$	0.6
$g11$	0.5
$g12$	0.3
$g13$	0.2
$g14$	0.9

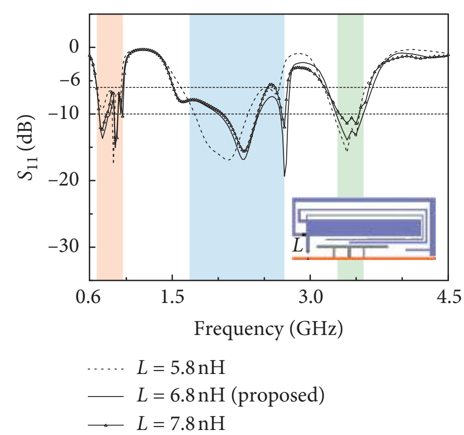

FIGURE 3: Simulated S_{11} as a function of the value inductor L for the proposed antenna.

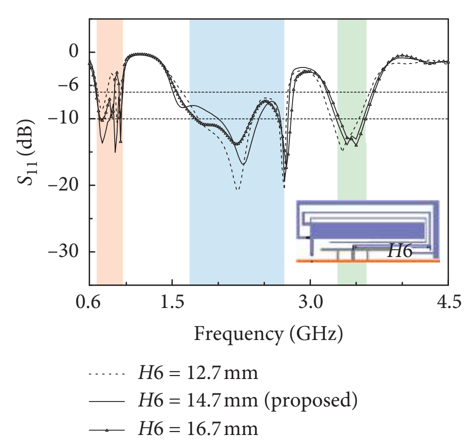

FIGURE 4: Simulated S_{11} as a function of the length $H6$ for the proposed antenna.

along the shorter strip (E-F-N), which can provide a 0.25-wavelength resonant mode at 2300 MHz (for M_2).

The simulated surface current distribution at 2730 MHz for the antenna is plotted in Figure 7(c), in which intense current

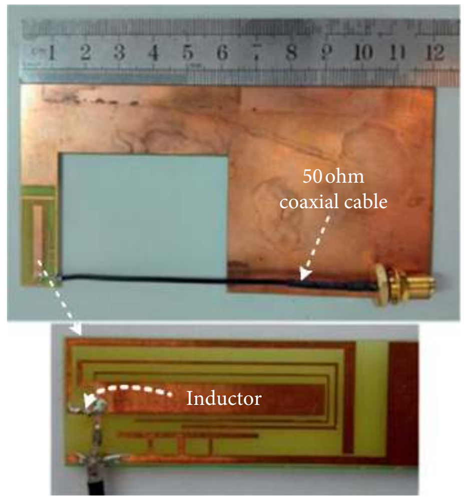

Figure 5: Photograph of the antenna.

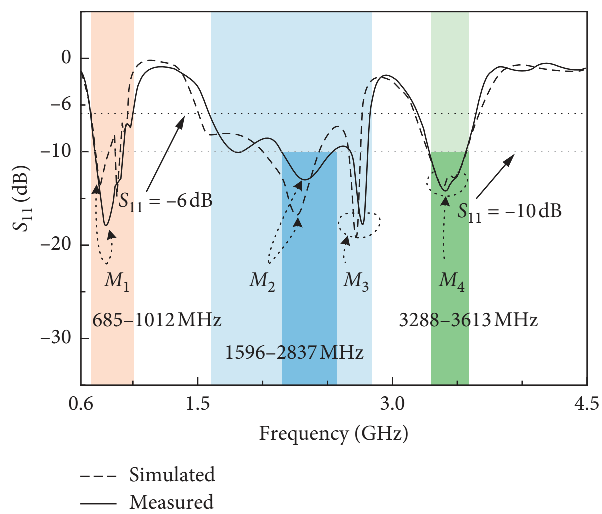

Figure 6: Simulated and measured S_{11} of the proposed antenna.

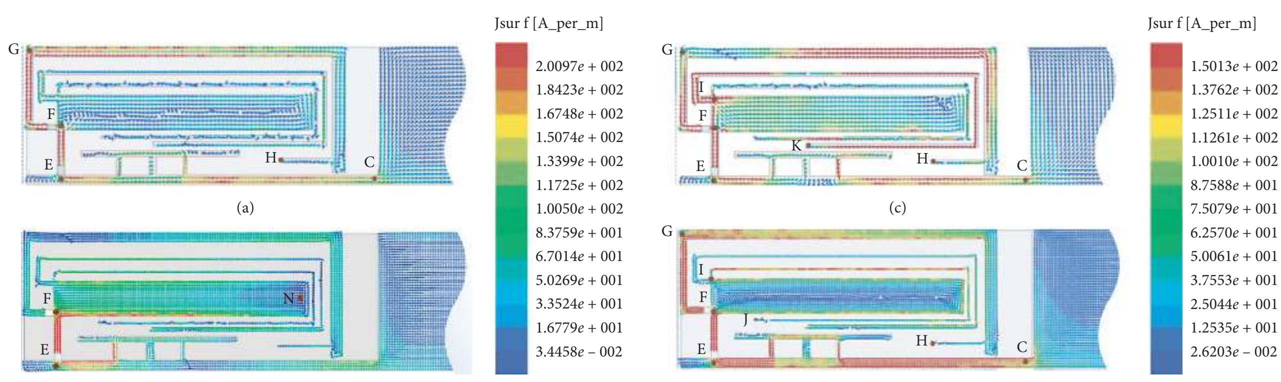

Figure 7: Simulated current distributions on metallic radiators of the proposed antenna at (a) 740 MHz, (b) 2300 MHz, (c) 2730 MHz, and (d) 3450 MHz.

distributions can be observed around the paths E-F-G-H, E-F-I-K, and E-C. That occurs because the paths E-F-G-H, E-F-I-K, and E-C operate at 0.25-wavelength mode (for M_3).

Moreover, Figure 7(d) shows that the fundamental mode is excited at 3450 MHz with maximum strength along the meandered arm (E-F-G-H and E-I-J) and the

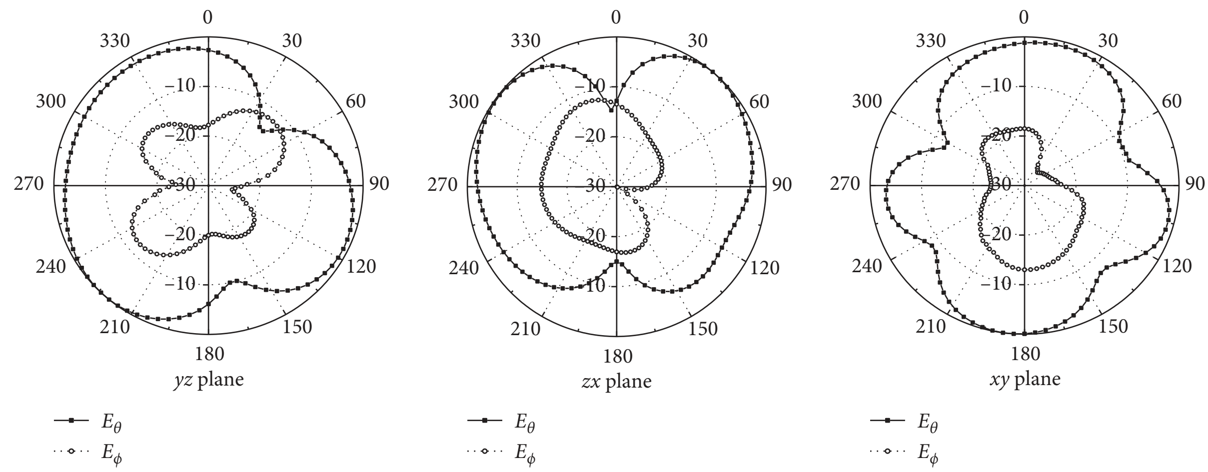

(a)

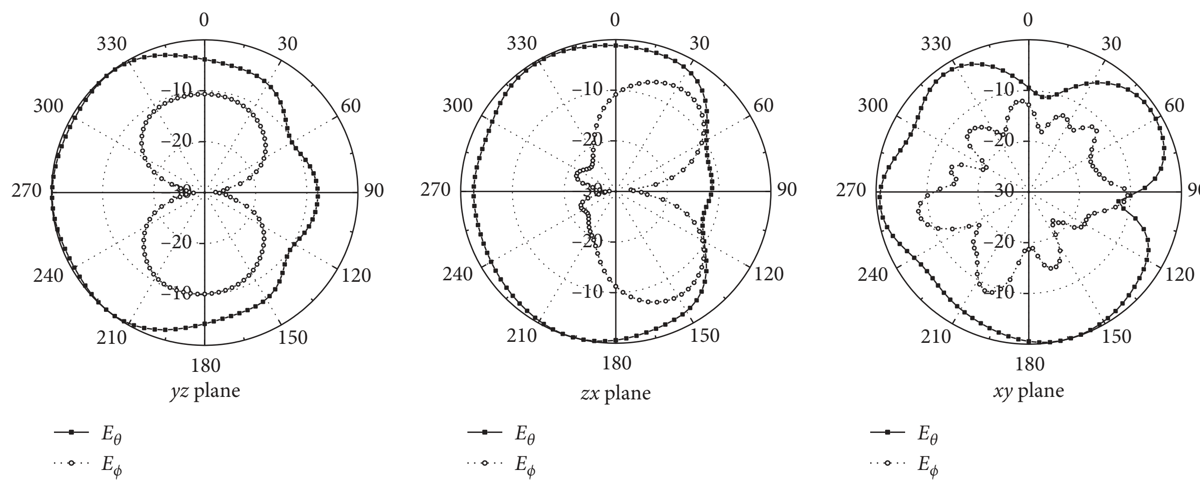

(b)

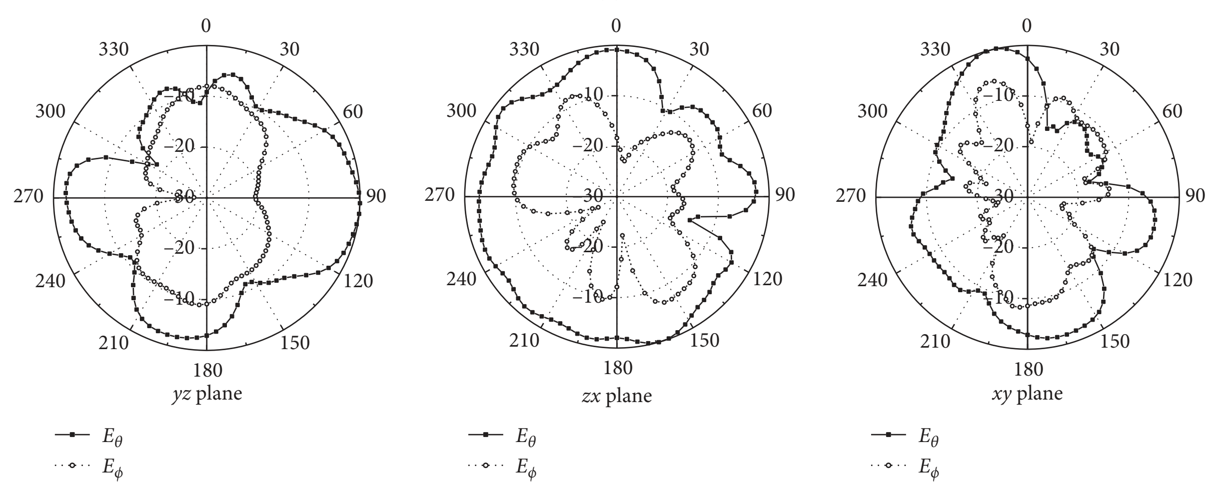

(c)

Figure 8: Continued.

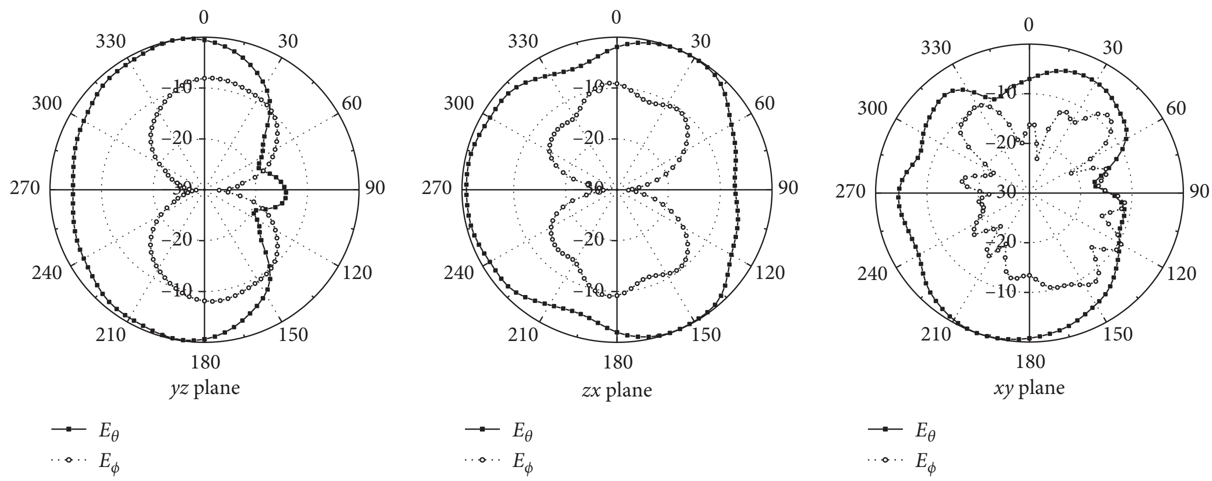

(d)

Figure 8: Measured radiation patterns of the proposed antenna at (a) 750 MHz, (b) 1800 MHz, (c) 2500 MHz, and (d) 3450 MHz.

staircase-shaped coupled ground strip (E-C), which works at the 0.25-wavelength mode of the strip section at 3450 MHz (for M_4).

Figure 8 shows the measured radiation patterns of the proposed antenna at 750, 1800, 2500, and 3450 MHz. Based on the direction of the antenna placement in Figure 1, the copol (E_θ) and crosspol (E_ϕ) in the *yoz*, *zox*, and *xoy* planes are measured. As can be seen from Figure 8, E_θ varies smoothly in *yoz* and *zox* planes which presented omnidirectional radiation. At 750 MHz, the E_θ radiation pattern appears as a figure-8 shape and is stronger than the E_ϕ radiation pattern. More variations can be observed in the radiation patterns at the *xoy* plane, but this radiation has little influence on the proposed antenna's overall characteristics. By comparing E_θ and E_ϕ in the analysis table, the proposed antenna exhibits remarkable characteristics of directivity and polarization which can meet the requirement of antenna directionality.

The measured antenna gain and radiation efficiency of the fabricated antenna are shown in Figure 9. Within the desired LTE700/GSM850/900 bands, i.e., 704–960 MHz, the measured antenna gain is about 1.4–1.9 dBi, and the corresponding radiation efficiency varies from 38% to 43%. Besides, for the middle operation band for DCS1800/PCS1900/UMTS2100 and LTE2300/2500 bands (1710–2690 MHz), the measured antenna gain is about 1.7–2.2 dBi, and the corresponding total radiation efficiency is larger than 40%. In the high band for 5G (3300–3600 MHz), the measured gain of the antenna varies from 2.2 to 2.5 dBi, and the radiation efficiency is from 45% to 47%. As a result, the measured efficiency and gain of the proposed antenna meet the requirement of the mobile phone systems.

Performances of the proposed antenna are compared with that of some typical mobile phones in terms of their frequency bands, dimensions, structures, and bandwidth in Table 2. In this table, we can find that the antennas in [9, 10]

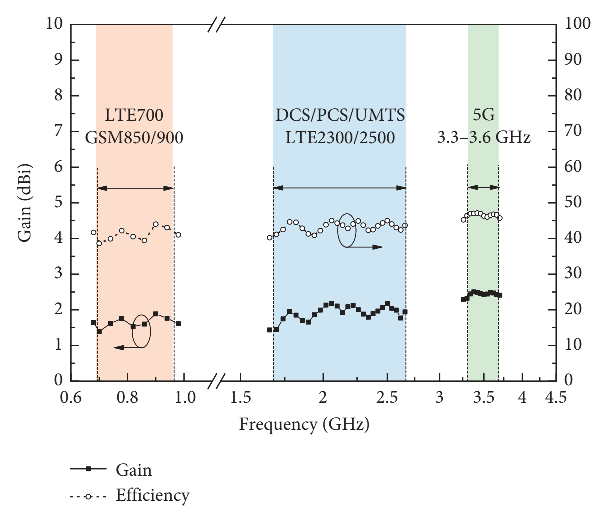

Figure 9: Measurement results for the gain and efficiency of the proposed antenna.

have a thin antenna thickness using the lumped elements, while the size of which is larger than that of the proposed antenna. The antennas in [4, 5] also have a thin antenna thickness, but they use double PCBs (printed circuit boards). The antennas in [1, 16] do not use any lumped elements, while suffering from a thickness of greater than 5 mm. The areas of antennas in [8, 15] are larger than that of the proposed antenna, and they do not cover the LTE700 band, which is the most difficult to be covered and crucial for LTE/WLAN (Wireless Local Area Networks) mobile phones. However, the proposed antenna can cover three frequency bands (685–1012 MHz, 1596–2837 MHz, and 3288–3613 MHz), furthermore S_{11} lower than −10 dB inside the operation bandwidths of WLAN (2400–2484 MHz) and 5G (3300–3600 MHz). This antenna has smaller size and single-layer structure than other multiple resonance antennas in literatures.

Table 2: Comparison of the proposed antenna and reference antennas.

Reference	Frequency band[a]	Dimension (mm^3)	Structure	Bandwidth (MHz)	S_{11} (dB)
[1]	Octa-band	$80 \times 6 \times 5.8$	Multilayer	670–1020/1650–2920	−6
[4]	Octa-band	$60 \times 15 \times 0.8$	Double layer	740–965/1380–2703	−6
[5]	Nona-band	$60 \times 10 \times 0.8$	Double layer	698–960/1710–2170	−6
[8]	Hepta-band	$70 \times 8 \times 5$	Multilayer	824–960/1710–2690	−6
[9]	Octa-band	$36.5 \times 10 \times 1.6$	Single layer	790–1030/1710–2230	−6
[10]	Hepta-band	$28 \times 15 \times 4$	Multilayer	808–965/1696–3000	−6
[15]	Hepta-band	$60 \times 5 \times 5$	Multilayer	760–960/1510–2720	−6
[16]	Octa-band	$70 \times 8 \times 5.8$	Multilayer	690–970/1680–2740	−6
Proposed	Deca-band	$27 \times 10.8 \times 0.8$	Single layer	685-1012/1596-2837/3288-3613	−6 and −10

[a]Hepta-band: GSM850/900/DCS/PCS/UMTS/LTE2300/2500. Octa-band: LTE/WWAN. Nona-band: LTE/WWAN/WLAN. Deca-band: LTE/WWAN/WLAN/5G (3300–3600 MHz).

5. Conclusion

A compact wideband printed antenna for deca-band operation is proposed. The antenna is formed by merging four strips, a staircase-shaped coupled ground strip and an inductor which can provide three wide bandwidths of 685–1012 MHz, 1596–2837 MHz, and 3288–3613 MHz. These bands can cover the standard LTE700/2300/2500, GSM850/900, DCS, PCS, UMTS, 2.4 GHz WLAN, and 5G (3300–3600 MHz). Furthermore, good efficiency of more than 38% and peak gains from 1.4 dBi to 2.5 dBi are achieved across the three bands. The measured results indicate that the proposed antenna is suitable for the applications in mobile phones for LTE/4G/5G/WLAN operations.

Data Availability

The data used to support the findings of this study are available from the corresponding author upon request.

Conflicts of Interest

The authors declare that they have no conflicts of interest.

Acknowledgments

This work was supported by the National Natural Science Foundation of China under Grant no. 61172020 and the Key Program in the Youth Elite Support Plan in Universities of Anhui Province under Grant no. gxyqZD2016521.

References

[1] D. Huang, Z. Du, and Y. Wang, "An octa-band monopole antenna with a small non-ground portion height for LTE/WLAN mobile phones," *IEEE Transactions on Antennas and Propagation*, vol. 65, no. 2, pp. 878–882, 2017.

[2] P. Wang, Y. Shao, D. Huang, and M. A. Basit, "A compact coupled-fed loop antenna for mobile LTE smartphones," *International Journal of Antennas and Propagation*, vol. 2018, Article ID 8426574, 8 pages, 2018.

[3] H. Xu, H. Wang, S. Gao et al., "A compact and low-profile loop antenna with six resonant modes for LTE smartphone," *IEEE Transactions on Antennas and Propagation*, vol. 64, no. 9, pp. 3743–3751, 2016.

[4] J. Dong, X. Yu, and L. Deng, "A decoupled multiband dual-antenna system for WWAN/LTE smartphone applications," *IEEE Antennas and Wireless Propagation Letters*, vol. 16, pp. 1528–1532, 2017.

[5] Y. Liu, P. Q. Liu, Z. J. Meng, L. F. Wang, and Y. Li, "A planar printed nona-band loop-monopole reconfigurable antenna for mobile handsets," *IEEE Antennas and Wireless Propagation Letters*, vol. 17, no. 7, pp. 1575–1579, 2018.

[6] Z. Yu, J. Yu, X. Ran, and C. Zhu, "A novel Koch and Sierpinski combined fractal antenna for 2G/3G/4G/5G/WLAN/navigation applications/4G/5G/WLAN/navigation applications," *Microwave and Optical Technology Letters*, vol. 59, no. 9, pp. 2147–2155, 2017.

[7] Y.-L. Ban, Y.-F. Qiang, G. Wu, H. Wang, and K.-L. Wong, "Reconfigurable narrow-frame antenna for LTE/WWAN metal-rimmed smartphone applications," *IET Microwaves, Antennas & Propagation*, vol. 10, no. 10, pp. 1092–1100, 2016.

[8] Y. Liu, Y.-M. Zhou, G.-F. Liu, and S.-X. Gong, "Heptaband inverted-F antenna for metal-rimmed mobile phone applications," *IEEE Antennas and Wireless Propagation Letters*, vol. 15, pp. 996–999, 2016.

[9] S. W. Lee and Y. Sung, "Compact frequency reconfigurable antenna for LTE/WWAN mobile handset applications," *IEEE Transactions on Antennas and Propagation*, vol. 63, no. 10, pp. 4572–4577, 2015.

[10] Y. Xu, Y.-W. Liang, and H.-M. Zhou, "Small-size reconfigurable antenna for WWAN/LTE/GNSS smartphone applications," *IET Microwaves, Antennas & Propagation*, vol. 11, no. 6, pp. 923–928, 2017.

[11] D. Huang and Z. Du, "Eight-band antenna with a small ground clearance for LTE metal-frame mobile phone applications," *IEEE Antennas and Wireless Propagation Letters*, vol. 17, no. 1, pp. 34–37, 2018.

[12] H. Chen and A. Zhao, "LTE antenna design for mobile phone with metal frame," *IEEE Antennas and Wireless Propagation Letters*, vol. 15, pp. 1462–1465, 2016.

[13] L.-W. Zhang, Y.-L. Ban, C.-Y.-D. Sim, J. Guo, and Z.-F. Yu, "Parallel dual-loop antenna for WWAN/LTE metal-rimmed smartphone," *IEEE Transactions on Antennas and Propagation*, vol. 66, no. 3, pp. 1217–1226, 2018.

[14] K.-L. Wong and C.-Y. Tsai, "IFA-based metal-frame antenna without ground clearance for the LTE/WWAN operation in the metal-casing tablet computer," *IEEE Transactions on Antennas and Propagation*, vol. 64, no. 1, pp. 53–60, 2016.

[15] Y. Yang, Z. Zhao, W. Yang, Z. Nie, and Q.-H. Liu, "Compact multimode monopole antenna for metal-rimmed mobile phones," *IEEE Transactions on Antennas and Propagation*, vol. 65, no. 5, pp. 2297–2304, 2017.

[16] R. Tang and Z. Du, "Wideband monopole without lumped elements for octa-band narrow-frame LTE smartphone," *IEEE Antennas and Wireless Propagation Letters*, vol. 16, pp. 720–723, 2017.